Journal of Materials Chemistry B

Accepted Manuscript

ROYAL SOCIETY OF CHEMISTRY

www.rsc.org/materialsB

Journal of Materials Chemistry B

Cite this: DOI: 10.1039/c0xx00000x

www.rsc.org/xxxxxx

FULL PAPER

Fabrication of a simple and sensitive QDs-based electrochemiluminescence immunosensor using a nanostructured composite material for detection of tumor markers alpha-fetoprotein

Guangming Nie,* Chenxi Li, Lin Zhang and Ling Wang

Received (in XXX, XXX) Xth XXXXXXXXX 20XX, Accepted Xth XXXXXXXXX 20XX
DOI: 10.1039/b000000x

A simple and sensitive label-free QDs-based electrochemiluminescence (ECL) immunosensor for detecting tumor markers alpha-fetoprotein is reported. This probe is fabricated using a nanostructured composite material (PICA-MWNT) obtained by direct electrodeposition of indole-6-carboxylic acid (ICA) monomer and carboxylic groups ended multiwall carbon nanotubes (MWNTs) in one step. The obtained composite material with 2-aminoethanethiol modified CdSe nanoclusters as luminescent particles has larger surface area and quite a few functionalized carboxylic acid groups. Thus, QDs/PICA-MWNT will probably display good biocompatibility, high ECL intensity and stability, which is promising for the enhancement of detection signals and synergistic improvement of sensitivity. The ECL signals are logarithmically linear with the concentration of alpha-fetoprotein in a wide determination range from 0.002 to 2000 ng mL^{-1}, and the corresponding detection limit was 0.4 pg mL^{-1}. This proposed ECL sensor exhibits high stability, good selectivity and reproducibility, which offers a new insight into the fabrication of immunoassays for detecting other relevant biomarkers and has the potential for reliable point-of-care diagnostics of tumor or other diseases.

1. Introduction

Sensitive and reliable point-of-care detection of tumor markers is crucial essentially for the early clinic diagnosis and detection of cancer since the abnormal concentration of tumor markers in adult serum can be an early indication of some cancerous diseases. In recent years, immunological assays based on the highly specific antigen-antibody recognition have attracted considerable attentions and efforts in the detection of tumor markers[1]. The traditional immunoassays are usually exploiting enzyme-amplified conjugates as labels[2-4], which demands for sophisticated procedures and qualified personnel equipped with physiologically irrelevant binding information, thus gives rise to the consumption of labor, time and cost. By contrast, the label-free strategies are simple, rapid, and low-cost by directly monitoring the interfacial alteration of physical quantity such as surface plasmon resonance (SPR)[5], quartz crystal microbalance (QCM)[6], or electrochemical impedance spectroscopy (EIS)[7]. Numerous attempts have been made to improve the simplicity, selectivity and sensitivity of the label-free immunosensors.

Electrochemiluminescence (ECL), derived from chemiluminesence, has attracted particular interests in the field of biosensing application due to its inexpensive, excellent selectivity, high sensitivity and wide range of analytes[8,9]. In terms of the luminophor categories, ECL systems can be generally divided into organic systems (e.g., luminol), inorganic systems quantum dots (QDs) systems and (e.g., $Ru(bpy)_3^{2+}$)[10], among which QDs has become more and more fascinating for the construction of ECL biosensors due to its remarkable optical, electrical, electrochemical and luminescent properties[11-13]. The primary challenge QDs-based ECL immunosensors, however, is to find the valid interface between the protein and the electronic transducer.

Conducting polymers (CPs), which are not only used as immobilization carriers but also play an active role in the signal transduction of biosensors, have shown great promise for the application of biosensing by virtue of their unusual properties such as rapid electron transfer, specificity, high sensitivity and biocompatibility[14-18]. Compared to pure CPs, the composites of CPs with nanomaterials including nanoparticles or carbon nanotubes (CNTs), typically have higher surface area, lower charge transfer resistance and mass transfer impedance, and have been successfully employed as sensing elements in biosensors[19-21]. CNTs are unique one-dimensional nanostructures with high porosity and reactivity, along with large active surface area, making it one of the most promising nanosupport for biomolecule immobilization[22-24]. Usually, the CNTs-modified electrodes are prepared by dispersing the CNTs solution onto electrode surface[25]. CNTs are, nevertheless, disordered on the electrode and apt to peel off from the electrode surface, which leads to the difficulties in achieving detection reproducibility[26]. Besides, some researchers came up with preparing the composites of CPs/CNTs by physical incorporation of CNTs[27]. Yet, the lack of chemical compatibility between the CPs and CNTs has made it hard to disperse CNTs into the polymer matrix[28].

State Key Laboratory Base of Eco-chemical Engineering, College of Chemistry and Molecular Engineering, Qingdao University of Science and Technology, Qingdao 266042, People's Republic of China.
Fax: +86 532 88957187; Tel: +86 532 88956556, E-mail: gmnie@126.com

Electropolymerization is one of the most convenient methods to prepare thin CPs film[29]. Our group have prepared a simple label-free electrochemical DNA sensor with detection limit of 5.79 pmol L^{-1} based on a novel nanostructured conducting poly(indole-6-carboxylic acid) obtained by electrochemical polymerization[30]. It is a fact that carboxylic groups can impart negative charges on CNTs, thus helping anionic CNTs act as a strong and conductive dopant during the electropolymerization. CNTs can also enhance the ECL of QDs by reducing the injection barrier of electrons to QDs. As the polypyrrole[31] and polythiophene[32,33] derivatives have been the most commonly investigated CPs for biosensor applications, our group is currently concerned with the polyindole family considering its several advantages, especially fairly good thermal stability, photoelectric property, high redox activity and stability[34,35].

Based on these considerations, we prepared a nanostructured composite material (PICA-MWNT) by direct electrochemical polymerization indole-6-carboxylic acid (ICA) and carboxylic groups ended multiwalled carbon nanotubes (MWNTs) as a dopant in electrodeposition. In addition, the PICA-MWNT composite has larger surface area and quite a few functionalized carboxylic acid groups. Thus, QDs/PICA-MWNT will probably display good biocompatibility, high ECL intensity and stability, which is promising for the enhancement of detection signals and synergistic improvement of sensitivity.

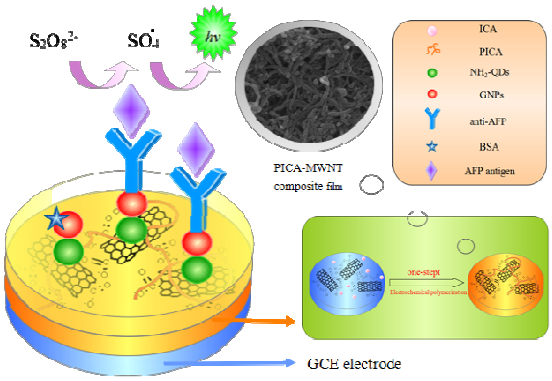

Scheme 1. The fabricating steps of the label-free ECL immunosensor based on PICA-MWNT composite with CdSe QDs as luminescent particles and SEM image of PICA-MWNT composite film

Herein, we proposed a simple label-free ECL immunosensor for detection of alpha-fetoprotein (AFP) based on the PICA-MWNT composite with 2-aminoethanethiol modified CdSe nanoclusters as luminescent particles (Scheme 1). Gold nanoparticles (GNPs) were combined with CdSe/PICA-MWNT to further amplify the ECL signals, and antibody (anti-AFP) was linked to the GNPs/CdSe/PICA-MWNT composite film via Au-N bond[36-38]. This design was much simpler than that with $Ru(bpy)_3^{2+}$ [39] or based rolling circle amplification (RCA) strategy[40]. Our group have reported a simple CdSe ECL sensor based on the PICA-MWNTs composite material, this sensor shows high sensitivity and good selectivity for Ramos cells with a low detection limit of 390 cells mL^{-1} [41]. This result provides a successful example, hence, we try to take advantage of the excellent properties of nanostructured composite material, CdSe QDs and gold nanoparticles fabrication immunosensor for AFP detection. This ECL immunoassay provides a convenient, low cost and sensitive for AFP detection, which shows greater potential in the clinic diagnose and clinical practice than previous CdSe ECL sensor.

2. Experimental section

2.1 Chemicals and materials

Indole-6-carboxylic acid (ICA, Aldrich, 98%) was used as received. Carboxylic groups ended multiwalled carbon nanotubes (MWNTs, Chengdu Organic Chemicals Co. Ltd., 95%) were used as received. Tetrabutylammonium tetrafluoroborate (TBATFB, Acros Organics, 95%) was dried in vacuum at 60 ◦C for 24 h before use. Commercial HPLC grade acetonitrile (ACN, made by Tianjin Guangfu Fine Chemical Research Institute, China) was used directly without further purification. 1-Ethyl-3-(3-dimethyl aminopropyl)carbodiimide (EDC) and N-hydroxysuccinimide (NHS) were obtained from Sigma and used without further purification. The standard solutions of alpha-fetoprotein (AFP) were purchased from Zhengzhou Bosai Bio-tech Co. (China). Bovine serum albumin (BSA, 96-99%) was obtained from Sigma (St. Louis, MO, USA). Chloroauric acid ($HAuCl_4$) and trisodium citrate were obtained from Shanghai Reagent Company (Shanghai, China). Clinical serum samples were made available by The Affiliated Hospital of Qingdao University Medical College, China. Other chemicals were of analytical grade and used without further purification. The 0.1 M phosphate buffer solutions (PBS) at various pH values with 0.1 M $K_2S_2O_8$ and 0.1 M KCl as the electrolytes were prepared by mixing the stock solutions of 0.1 M NaH_2PO_4 and 0.1 M Na_2HPO_4 at different volume ratio. Double-distilled water (DDW) was used throughout the study.

2.2 Instrumentation

Electropolymerization of PICA-MWNT composite was carried out in a one compartment cell by using of a Model 263 potentiostat-galvanostat (EG&G Princeton Applied Research). The ECL emission was detected by a model MPI-A electrochemiluminescence analyzer (Xi'An Remax Electronic Science & Technology Co. Ltd., Xi'An, China) at room temperature. The voltage of the photo multiplier tube (PMT) was 600-700 V in the detection process. The working and counter electrodes were glass carbon electrode (GCE, 3.0 mm in diameter, 7.0 mm^2 in geometrical area) and platinum-wire electrode, respectively. The reference electrode was Ag/AgCl/KCl (KCl was the saturated solution). UV-visible spectra were taken by using Cary 50 UV-vis-NIR spectrophotometer. The fluorescence spectra were determined with Perkin-Elmer LS-55 fluorescence spectrophotometer. Transmission electron microscopy (TEM) measurements were taken with JEM-2000EX/ASID2. Scanning electronmicroscopy (SEM) measurements were taken by using a JEOL JSM-6700F scanning electron microscope.

2.3 Preparation of 2-aminoethanethiol modified CdSe QDs

Colloidal CdSe nanocrystals were prepared as described in references[42-44] with a slight modification. Briefly, freshly prepared 0.1 M NaHSe solution was added to 1.25 × 10^{-3} M saturated $CdCl_2$ solution at pH 5.6-5.9 in the presence of 2-aminoethanethiol (AET) as a stablilizing agent. Satisfying results were obtained when the molar ratio of Cd^{2+}/AET/HSe^- was fixed at 1:2.4:0.5. After being vigorously stirred for 10 min, the mixture was refluxed for 3 h to control the growth of CdTe nanocrystals.

2.4 Preparation of gold nanoparticles (GNPs)

Gold nanoparticles (GNPs) were prepared according to the method reported previously with a slight modification[45]. $HAuCl_4$ and trisodium citrate solutions were filtered through a 0.22 μm microporous membrane filter prior to use, and then 2 mL of 1% trisodium citrate was added to 50 mL of boiling 0.01% $HAuCl_4$ solution and stirred for 20 min at the boiling point. The prepared colloid gold nanoparticles were stored in brown glass bottles at 4 °C.

2.5 Electrodeposition of PICA-MWNT and PICA/MWNT composite material

Prior to electropolymerization, the working electrode surface was polished with 1.0 μm, 0.3 μm and 0.05 μm alumina slurry in sequence, then rinsed with DDW after each polishing step, and finally cleaned ultrasonically in water and 95% ethanol.

The PICA/MWNT composite was prepared by dropping 20 μL of 2 mg mL^{-1} MWNTs dispersed in ACN that was pretreated by ultrasonication for 40 min onto GCE surface, then the electropolymerization of PICA on the MWNT/GCE was carried out in the electrolyte of ACN containing 0.05 mol L^{-1} ICA monomer and 0.10 mol L^{-1} TBATFB. The PICA-MWNT composite was obtained from 0.05 mol L^{-1} ICA monomer and 2 mg mL^{-1} MWNTs in ACN, in which MWNTs was acted as supporting electrolyte.

All solutions were deaerated by a dry argon stream and maintained at a slight argon overpressure during experiments. The thickness of composite deposited on the electrode was controlled by the integrated charge passed through the cell. In order to remove the electrolyte and oligomers/monomers, the PICA-MWNT and PICA/MWNT composite film was rinsed with acetone firstly and finally DDW.

2.6 Fabrication of the ECL immunosensor

Firstly, 20 μL of EDC/NHS solution prepared by mixing 3 mM EDC and 5 mM NHS at a volume ratio of 1:1 before use was injected onto the PICA-MWNT composite, and the electrode was kept at 26 °C for 1 h. After rinsed with pH 7.4 PBS, 20 μL of 2-Aminoethanethiol modified CdSe QDs was dropped onto the surface of the electrode for 2 h at room temperature, followed by dripping 20 μL of GNPs onto the obtained CdSe/PICA-MWNT/GCE for another 2 h. Then the produced GNPs/CdSe/PICA-MWNT/GCE was dipped in 0.5 mg mL^{-1} anti-AFP solution (50 mM PBS, pH 7.4) at 4 °C for at least 12 h. Finally, it was incubated in 20 μL of 2 wt % BSA at 37 °C for 1 h to block nonspecific binding sites.

2.7 ECL Detection of AFP antigen

The ECL immunosensor anti-AFP/GNPs/CdSe/PICA-MWNT/GCE was incubated in 40 μL of AFP antigen solution at 37 °C for 50 min to form the antigen-antibody immunoconjugates. Then, the immunosensing electrode was scanned from 0 to -1.5 V in 0.1 M PBS (pH 7.4) containing 0.1 M $K_2S_2O_8$ and 0.1 M KCl. Thus, the label-free detection of AFP could be realized by measuring the changes of ECL signals before and after the immunological reaction.

3. Results and discussion

3.1 Characterization of PICA-MWNT composite material

Larger surface area and better charge transport property is an important factor for the CPs-CNTs modified immunoelectrode. Fig. 1 showed the SEM image of the morphology and microstructure of the MWNTs and deposited film. As can be seen Fig. 1A, different length of MWNTs are bound to each other, the diameter is between 20-30 nm, and the purity of MWNTs is very high. The PICA/MWNT composite film was shown in Fig. 1B, the PICA/MWNT composite film is compact and resembles arrangements of rods with 80-100 nm diameter in the form of fibrillar network. By contrast, PICA-MWNT composite material (Fig. 1C) represented an extremely homogeneous and intact fiber-shaped nanostructure owing to the well-dispersedness and incorporation of MWNTs in the composite layer. On the other hand, the nano-meter pores within the composite film could provide more pathways for the movement of ions and solvent molecules, thus lead to better electrochemical properties than PICA/MWNT composite film and the pure PICA film[46]. In conclusion, the PICA-MWNTs composite material was an ideal candidate for the fabrication of immunosensor based on CPs-CNTs composite.

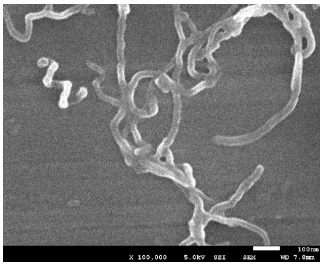

(A)

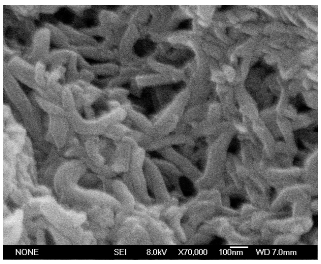

(B)

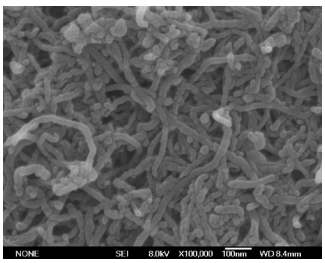

(C)

Fig. 1 SEM image of (A) MWNTs, (B) PICA/MWNT and (C) PICA-MWNT composite film.

3.2 Characterization of 2-aminoethanethiol modified CdSe QDs and GNPs

Fig. 2A showed the UV-vis absorption spectrum and TEM image of the prepared GNPs. As shown in Fig. 2A, the GNPs revealed

the absorption peak at 519 nm, and had an average diameter of approximately 15 nm according to the TEM image (inset, Fig. 2A).The UV-vis absorption (curve a) and the photoluminescence (PL) spectra (curve b) of the prepared 2-Aminoethanethiol modified CdSe QDs were shown in Fig. 2B. It can be seen that

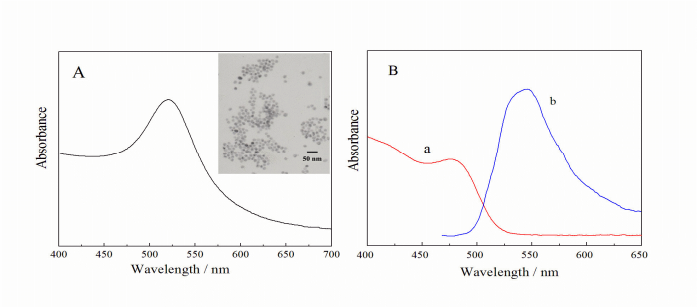

the UV-vis absorption peak and PL peak occurred at 478 nm and 554 nm, respectively.

Fig. 2 (A) UV-vis absorption spectrum of the gold nanoparticles (GNPs), inset: transmission electron microscopy (TEM) of the GNPs. (B) UV-vis absorption spectra (curve a) and Photoluminescence (PL) (curve b) of the CdSe QDs in aqueous solution (excitation wavelength: 400 nm).

The particle size of CdSe QDs was calculated to be 14 nm on the basis of the empirical equation reported previously[47].

CdSe: $D = (1.6122 \times 10^{-9})\lambda^4 - (2.6575 \times 10^{-6})\lambda^3 + (1.6242 \times 10^{-3})\lambda^2 - 0.4277\lambda + 41.57$

In the above equation, D (nm) is the diameter of CdSe QDs, and λ (nm) is the wavelength of the first excitonic absorption peak of the UV-vis absorption spectrum.

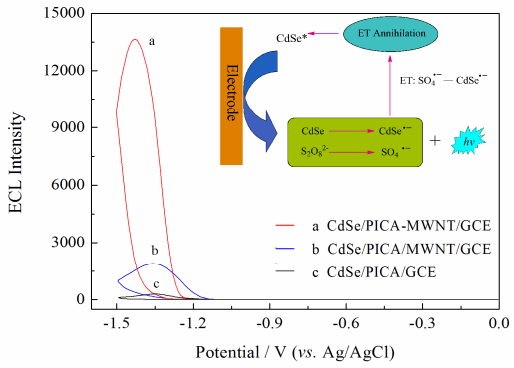

3.3 ECL behaviors of the CdSe QDs on the PICA-MWNT composite

Fig. 3 ECL-potential curves of (a) the CdSe/PICA-MWNT modified electrode, (b) CdSe/PICA/MWNT modified electrode and (c) the CdSe/pure PICA modified electrode in 0.1 M PBS (pH 7.5) containing 0.1 M KCl and 0.1 M $K_2S_2O_8$. Inset: the mechanism of ECL of CdSe QDs on the PICA-MWNT composite.

To investigate the MWNT-amplification for ECL measurement, the ECL of CdSe/PICA-MWNT was compared with pure CdSe/PICA film and CdSe/PICA/MWNT film (Fig. 3). In

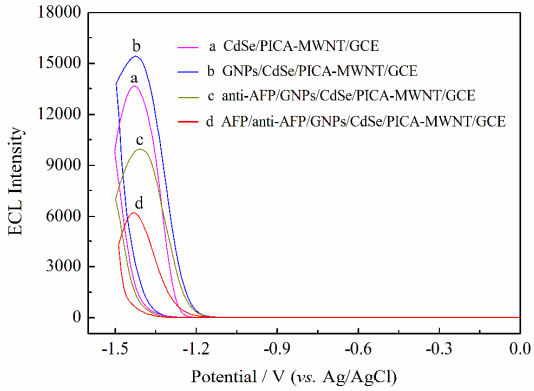

comparison, PICA/MWNT composite was prepared by dropping MWNTs onto GCE surface, then electrodeposition of PICA on the MWNT/GCE was carried out. As shown in Fig. 3, the ECL

Fig. 4 ECL-potential curves of (a) CdSe/PICA-MWNT composite, (b) GNPs/CdSe/PICA-MWNT composite, (c) anti-AFP/GNPs/CdSe/PICA-MWNT composite, (d) AFP/anti-AFP/GNPs/CdSe/PICA-MWNT composite modified electrodes in 0.1 M PBS (pH 7.5) containing 0.1 M KCl and 0.1 M $K_2S_2O_8$ (the voltage of the photomultiplier tube was set at 600 V). Scan rate: 100 mV s^{-1}.

intensity of CdSe/PICA-MWNT composite modified electrode(curve a), where the ECL peak was observed at -1.4 V, was about 26 fold higher than that observed on the pure CdSe/PICA modified electrode (curve c) and 7 fold higher than that of CdSe/PICA/MWNT film modified electrode (curve b), indicating the nanostructure of the PICA-MWNT composite could amplify the ECL signal greatly. The reasonable explanation might be that the nano-meter porous structure, larger surface area and better conductivity of the PICA-MWNT composite film can acilitate the ECL reaction in the presence of CdSe QDs. Therefore, the CdSe/PICA-MWNT composite film was more favorable for the fabrication of the ECL immunosensor. The mechanism of the ECL reaction of CdSe on the PICA-MWNT composite modified GCE was illustrated in the inset of Fig. 3. Upon the potential scan with an initial negative direction, the CdSe QDs immobilized at the electrode were reduced to nanocrystal species ($CdSe^{\bullet-}$), while $S_2O_8^{2-}$ was reduced to the strong oxidant $SO_4^{\bullet-}$, which could react with the negatively charged $CdSe^{\bullet-}$ through electron transfer, producing the excited state ($CdSe^*$) to emit light in solution[48].

3.4 ECL characterizations of the modified electrodes

To characterize the fabrication process of the ECL immunosensor, ECL signals at each immobilization step were recorded in Fig. 4. When GNPs were assembled onto the CdSe/PICA-MWNT composite modified electrode (curve b) via Au-N bonds, the ECL signal was further improved (curve b). The reason might be that the GNPs played an important role similar to a conducting wire which promoted the electron transfer in the ECL reaction. When the antibody (anti-AFP) was immobilized onto the GNPs/CdSe/PICA-MWNT modified electrode, the ECL intensity decreased obviously (curve c). After the nonspecific binding sites were blocked by using bovine serum albumin (BSA), the

immunoreaction took place and the immunoconjugates formed. The ECL intensity showed a further decrease (curve d), indicating that the electron exchange in ECL reaction was blocked due to the increased spatial hindrance and impedance from the formed protein layer.

3.5 Optimization of reaction conditions

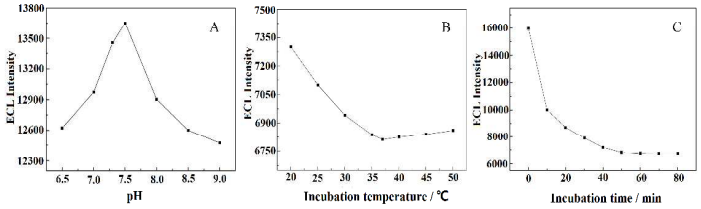

Fig. 5 Effects of (A) the buffer solution pH, (B) incubation temperature and (C) incubation time on the ECL response of the immunosensor.

The ECL reaction of the immunosensor could be affected by pH of the buffer solution, incubation temperature and incubation time. Therefore, the effects on pH of the buffer solution, incubation temperature and time were studied. The pH of the buffer solution influence on the ECL of the immunosensor was investigated in the range of 6.5-9.0. As shown in Fig. 5A, the ECL intensity increased gradually from 6.5 to 7.5. But when pH became higher than 7.5, ECL intensity of the immunosensor began to decrease obviously. Therefore, the pH 7.5 PBS was selected for the following ECL experiment. Fig. 5B showed the relationship between the incubation temperature and the ECL intensity. From 20 °C to 50 °C, the ECL intensity of the immunosensor reached a minimum value at 37 °C, suggesting that the maximum immunoreaction occurred at this temperature. The effect of incubation time on the immunoreaction was shown in Fig. 5C. The ECL intensity of the immunoelecrode gradually decreased with the increase of incubation time, and finally leveled off after 70 min, which indicated that the immunoreaction reached equilibrium. Thus, the optimum incubation time was chosen as 70 min.

3.6 Lable-free ECL detection of AFP with the immunosensor

Fig. 6 showed the ECL intensity of the immunosensor without the AFP under continuously scans for 6 cycles from 0 to -1.5 V. When the immunosensor was continuously scanned, stable and high ECL signals could be still observed, which meant that the immunosensor possessed potential cycling stability and was suitable for ECL detection.

As shown in Scheme 1, when the anti-AFP/GNPs/CdSe/PICA-MWNT/GCE was incubating with the AFP antigen, the non-conductive immunoconjugates was formed by the antigen-antibody reaction. Since the immunocomplexes formed in the immunoreaction could increase the spatial blocking and impedance and hinder the ECL reaction between CdSe QDs and $K_2S_2O_8$, the electron-transfer speed in the ECL reaction slowed down, and the ECL intensity decreased accordingly. Therefore, the AFP concentration could be determined with the fabricated ECL immunosensor based on a label-free strategy. When the immunosensor was continuously scanned, stable and high ECL signals could be still observed, which meant that the immunosensor possessed potential cycling stability and was

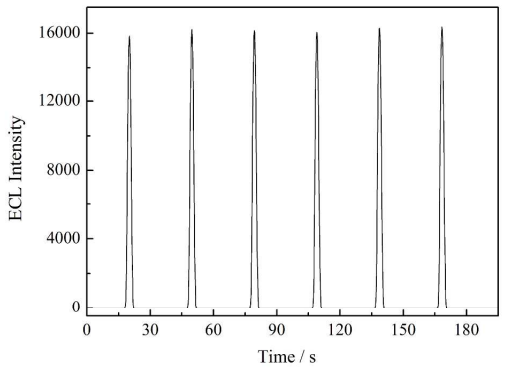

Fig. 6 Stability of anti-AFP/GNPs/CdSe/PICA-MWNT composite modified electrodes in 0.1 M pH 7.5 PBS. The scanning voltage range: -1.5 to 0 V, scan rate: 100 mV s^{-1}, PMT voltage: 700 V.

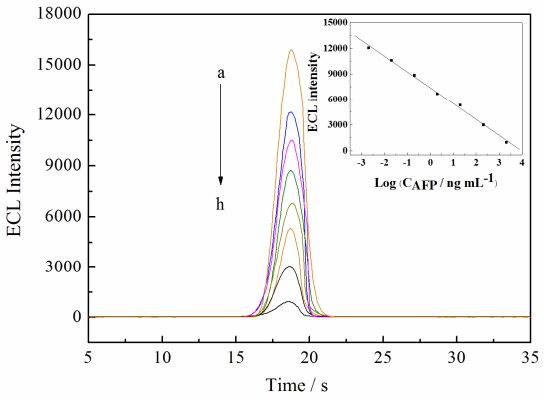

Fig. 7 ECL profiles of the immunosensor in the presence (a-h) of different concentrations of AFP in pH 7.5 PBS containing 0.1 M KCl and 0.1 M $K_2S_2O_8$. AFP concentration: (a) 0, (b) 0.002 (c) 0.02, (d) 0.2, (e) 2, (f) 20, (g) 200, (h) 2000 ng mL^{-1}. Inset: Linear calibration plots for AFP determination. Scan rate: 100 mV s^{-1}.

suitable for ECL detection. Under the optimal conditions, a series of ECL emissions obtained by incubating the immunosensor with different concentrations of AFP were shown in Fig. 7. Curve a was obtained by incubating the anti-AFP/GNPs/CdSe/PICA-MWNT/GCE in PBS (pH 7.5) containing 0.1 M KCl and 0.1 M $K_2S_2O_8$ in the absence of AFP. From curve b to curve h, it can be seen that the ECL intensities decreased with the increasing concentrations of AFP. The linear determination range for AFP was from 0.002 to 2000 ng mL^{-1} with a correlation coefficient of 0.9988 (Fig. 7, inset), the detection limit was 0.4 pg mL^{-1} according to 3σ. A series of eleven repetitive measurements of 0.2 ng mL^{-1} AFP were used for estimating the precision, the value of RSD was 8.6%. As shown in Table 1, this proposed ECL

immunosensor exhibited relative wider response range and higher sensitivity compared with previous reported.

Table 1. Comparison between the proposed strategy and other reported methods for alpha-fetoprotein detection

Detection method	Linear range	Detection limit	Ref.
This work	0.002–2000 ng mL^{-1}	0.4 pg mL^{-1}	–
Graphene sheet&carbon sphere	0.05-6 ng mL^{-1}	0.02 ng mL^{-1}	49
Collagen-TiO_2/nano-Au	10–60 ng mL^{-1}	29 pg mL^{-1}	50
TiO_2-graphene	0.1–300.0 ng mL^{-1}	0.03 ng mL^{-1}	51
MWCNTs/SiO_2	0.1–30.0 ng mL^{-1}	0.018 ng mL^{-1}	52
Fe_3O_4@Au	1.0–200.0 ng mL^{-1}	0.65 ng mL^{-1}	53
Silver–graphene	0.01–100 ng mL^{-1}	3 pg mL^{-1}	54
Pd/GCE	0.01–75.0 ng mL^{-1}	4 pg mL^{-1}	55

3.7 Specificity, stability, reproducibility and application of the immunosensor

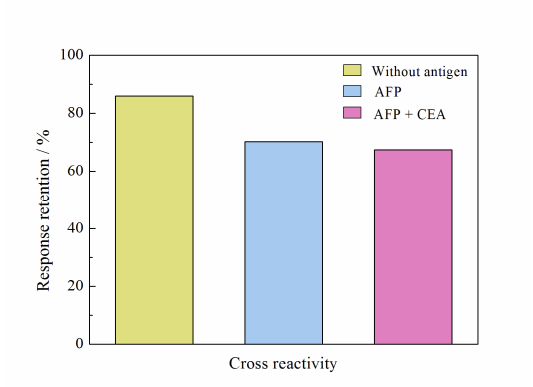

Fig. 8 Reserved percentage of the DPV responses for the determination of AFP after anti-AFP/GNPs/CdSe/PICA-MWNT/GCE incubating in the AFP solution (20 ng mL^{-1}) and the coexisting interference antigen solution of AFP (20 ng mL^{-1}) + CEA (10 ng mL^{-1}).

To investigate the specificity of the proposed immunosensor for AFP detection, we detected the ECL signals of the mixture containing 20 ng mL^{-1} AFP and 10 ng mL^{-1} carcinoembryonic antigen (CEA). No remarkable change of ECL signals was observed in comparison with the result obtained in the presence of AFP alone, indicating good specificity of the proposed ECL immunosensor, as show in Fig. 8. The stability of the immunosensor was measured by stored the immunosensor in pH 7.5 PBS at 4 °C over 30 days and no obvious change in the same AFP concentration was found, indicating that the proposed immunosensor had a good stability. AFP at the same concentration of 2 ng mL^{-1} were repeatedly detected by four electrodes of anti-AFP/GNPs/CdSe/PICA-MWNT/GCE prepared by the same procedure. Four measurements from the batch resulted in a relative standard deviation of 6.8%, demonstrating good reproducibility of the fabrication protocol.

The feasibility of this electrochemiluminescence immunosensor for clinical application was investigated on three real samples of human serum and the results were compared with ELISA. The results are summarized in Table 2. By comparison with the ELISA method, the recoveries from these two methods ranged from 98.4 to 101.5% and 99.4 to 103.0%, respectively. The relative deviation was lower than 2.0%. Satisfactory results were achieved, which also indicated this electrochemiluminescence immunosensor showed acceptable feasibility to detect AFP in human serum.

Table 2. Comparison assay results of human serum samples for the Proposed Method and ELISA

	proposed method (ng / mL)			ELISA (ng / mL)			
Sample	added	found	recovery (%)	added	found	recovery (%)	relative deviation (%)
1	0.02	0.0203	101.5	0.02	0.0206	103.0	-1.46
2	2.0	1.967	98.4	2.0	1.989	99.5	-1.11
3	200	201.9	101.04	200	198.8	99.4	1.61

4. Conclusions

In summary, we have successfully constructed a highly sensitive and simple ECL immunosensor for detecting cancer biomarkers alpha-fetoprotein (AFP) and demonstrated the signal amplification procedure. The greatly enhanced sensitivity relies upon a dual and synergic signal amplification scheme: (1) the nanostructure, larger surface area and better conductivity of the PICA-MWNT composite film facilitate the ECL reaction in the presence of CdSe QDs; (2) MWNTs can enhance the ECL performance of QDs by reducing the injection barrier of electrons to QDs; (3) the gold nanoparticles play an important role similar to a conductive wire facilitating the electron transfer in the ECL reaction. This proposed immunosensor possesses high sensitivity, good selectivity and reproducibility, which makes it a promising candidate for detecting other relevant biomarkers and has a potential application in the point-of-care diagnostics.

Acknowledgements

This work was supported by National Natural Science Foundation of China (51373089), NSF of Shandong (ZR2011BM003), Specialized Research Fund for the Doctoral Program of Higher Education (20123719120006), Scientific and Technical Development Project of Qingdao (11-2-4-3-(10)-jch).

Notes and references

1 B. V. Chikkaveeraiah, A. A. Bhirde, N. Y. Morgan, H. S. Eden and X. Y. Chen, *ACS. Nano*, 2012, **6**, 6546.

2 R. Malhotra, V. Patel, J. P. Vaqué, J. S. Gutkind and J. F. Rusling, *Anal. Chem.*, 2010, **82**, 3118.

3 S. Zang, Y. J. Liu, M. H. Lin, J. L. Kang, Y. M. Sun and H. T. Lei, *Electrochim. Acta.*, 2013, **90**, 246.

4 H. C. Yang, R. Yuan, Y. Q. Chai, L. Mao, H. L. Su, W. Jiang and M. Liang, *Biochem. Eng. J.,* 2011, **56**, 116.

5 D. E. P. Souto, J. V. Silva, H. R. Martins, A. B. Reis, R. C. S. Luz, L. T. Kubota and F. S. Damos, *Biosens. Bioelectron.*, 2013, **46**, 22.

6 C. Crosson and C. Rossi, *Biosens. Bioelectron.*, 2013, **42**, 453.

7 A. Ramanavicius, A. Finkelsteinas, H. Cesiulis and A. Ramanaviciene, *Bioelectrochemistry*, 2010, **79**, 11.

8 Z. Lin, F. Luo, Q. Liu, L. Chen, B. Qiu, Z. Cai and G. Chen, *Chem. Commun.*, 2011, **47**, 8064.

9 M. Yan, W. Gao, S. Ge, L. Ge, C. Chu, J. Yu, X. Song and S. Hou, *J. Mater. Chem.,* 2012, **22**, 5568.

10 10 G. Nie, Z. Bai, W. Yu and J. Chen, *Biomacromolecules*, 2013, **14**, 834.

11 Z. Y. Guo, T. T. Hao, S. Wang, N. Gan, X. Li and D. Y. Wei, *Electrochem. Commun.,* 2012, **14**, 13.

12 D. J. Lin, J. Wu, F. Yan, S. Y. Deng and H. X. Ju, *Anal. Chem.,* 2011, **83**, 5214.

15 13 W. R. Algar, A. J. Tavares and U. J. Krull, *Anal. Chim. Acta,* 2010, **673**, 1.

14 Y. Z. Long, M. M. Li, C. Z. Gu, M. X. Wan, J. L. Duvail, Z. W. Liu and Z. Y. Fan, *Prog. Polym. Sci.*, 2011, **36**, 1415.

15 G. Nie, L. Zhou, Q. Guo and S. Zhang, *Electrochem. Commun.,* 20 2010, **12**, 160.

16 A. Mulchandani and N. V. Myung, *Curr. Opin. Biotechnol.,* 2011, **22**, 502.

17 L. Xia, Z. X. Wei and M. X. Wan, *J. Colloid Interface Sci.,* 2010, **341**, 1.

25 18 S. Nambiar and J. T. W. Yeow, *Biosens. Bioelectron.,* 2011, **26**, 1825.

19 N. Roy, R. Sengupta and A. K. Bhowmick, *Prog. Polym. Sci.*, 2012, **37**, 781.

20 X. F. Lu, W. J. Zhang, C. Wang, T. C. Wen and Y. We, *Prog. Polym. Sci.,* 2011, **36**, 671.

30 21 Z. Gu, X. Y. Chen, Q. D. Shen, H. X. Ge and H. H. Xu, *Polymer,* 2010, **51**, 902.

22 L. Wang, Y. N. Liu, X. D. Yang, Y. Fang, Y. Z. Chen and B. P. Wang, *J. Mater. Chem. A*, 2013, **1**, 1834.

23 G. F. Gui, Y. Zhuo, Y. Q. Chai, N. Liao, M. Zhao, J. Han, Y. Xiang 35 and R. Yuan, *RSC Adv.*, 2014, **4**, 1955-1960.

24 S. Yi, S. Q. Tian, D. W. Zeng, K. Xu, S. P. Zhang and C. S. Xie, *Sens. Actuators, B,* 2013*,* **185***,* 345.

25 H. K. Maleh, P. Biparva and M. Hatami, *Biosens. Bioelectron.,* 2013, **48**, 270.

40 26 G. Z. Hu, L. Chen, Y. Guo and S. J. Shao, *Talanta,* 2009, **78**, 1211.

27 Y. G. Hu, Z. Y. Zhao and Q. Q. Wan, *Bioelectrochem.,* 2011, **81**, 59.

28 A. Peigney, E. Flahaut, C. Laurent, F. Chastel and A. Rousset, *Chem. Phys. Lett.*, 2002, **352**, 20.

29 B. Y. Lu, J. K. Xu, C. L. Fan, H. M. Miao and L. Shen, *J. Phys. Chem.* 45 *B,* 2009, **113**, 37.

30 G. Nie, Y. Zhang, Q. Guo and S. Zhang, *Sens. Actuat. B,* 2009, **139**, 592.

31 A. Baba, P. Taranekar, R. R. Ponnapati, W. Knoll and R. C. Advincula,

50 *ACS Appl. Mater. Interfaces,* 2010, **2**, 2347.

32 Y. Wen, J. Xu, M. Liu, D. Li, L. Lu, R. Yue and H. J. He, *Electroanal. Chem.,* 2012, **674**, 71.

33 L. Q. Qin, J. K. Xu, B. Y. Lu, Y. Lu, X. M. Duan and G. M. Nie, *J. Mater. Chem.,* 2012, **22**, 18345.

55 34 G. Nie, H. Yang, S. Wang and X. Li, *Crit. Rev. Solid State Mater. Sci.,* 2011, **36**, 209.

35 G. Nie, L. Zhou and Y. Yang, *J. Mater. Sci.*, 2011, **21**, 13873.

36 H. Zhang, M. Liu, G. Huang, Y. Yu, W. Shen and H. Cui, *J. Mater. Chem. B,* 2013, **1**, 970.

60 37 X. Liu, W. Li, L. Li, Y. Yang, L. Mao and Z. Peng, *Sens. Actuators B,* 2014, **191**, 408.

38 X. Jia, Z. Liu, N. Liu and Z. Ma, *Biosens. Bioelectron,* 2014, **53**, 160.

39 L. Ge, J. X. Yan, X. R. Song, M. Yan, S. G. Ge and J. H. Yu, *Biomaterials,* 2012, **33**, 1024.

65 40 B. Zhang, B. Q. Liu, J. Zhou, J. Tang and D. Q. Tang, *Appl. Mater.,* 2013, **5**, 4479.

41 G. Nie, Z. Bai, W. Yu and L. Zhang, *J. Polym. Sci., Part A: Polym. Chem.,* 2013, **51**, 2385

42 M. Y. Gao, S. Kirstein, H. Möhwald, A. L. Rogach, R. A. Kornowski, 70 A. Eychmüller and H. Weller, *J. Phys. Chem. B,* 1998, **102**, 8360.

43 X. S. Li, H. Billy and S. Matthias, *J. Am. Chem. Soc.*, 2006, **128**, 6278.

44 H. Zhang, Z. C. Cui, Y. Wang, K. Zhang, X. Ji, C. L. Lu, B. Yang and M. Y. Gao, *Adv. Mater.*, 2003, **15**, 777.

45 A. Ambrosi, M. T. CastaÇeda, A. J. Killard, M. R. Smyth, S. Alegret 75 and A. Merkoci, *Anal. Chem*., 2007, **79**, 5232.

46 ~~(a)G. Nie, Z. Bai, W. Yu and L. Zhang, *J. Polym. Sci., Part A: Polym. Chem.*, 2013, **51**, 2385; (b)~~ G. Nie, Z. Bai, J. Chen and W. Yu, *ACS Macro. Lett.,* 2012, **1**, 1304.

47 W. W. Yu, L. H. Qu, W. Z. Guo and X. G. Peng, *Chem. Mater.*, 2003, 80 **15**, 2854.

48 N. Myung, Z. Ding and A. J. Bard, *Nano Lett.*, 2002, **2**, 1315.

49 D. Du, Z. X. Zou, Y. Shin, J. Wang, H. Wu, M. H. Engelhard, J. Liu, I. A. Aksay and Y. H. Lin, *Anal. Chem*., 2010, **82**, 2989.

50 H. Su, R. Yuan, Y. Chai and Y. Zhuo, *Biosens. Bioelectron.*, 2012, 85 **33**, 288.

51 K. J. Huang, J. Li, Y. Y. Wu and Y. M. Liu, *Bioelectrochemistry*, 2013, **90**, 18.

52 R. P. Liang, Z. X. Wang, L. Zhang and J. D. Qiu, *Sensor. Actuat. B*, 2012, **166–167**, 569.

90 53 R. P. Liang, G. H. Yao, L. X. Fan and J. D. Qiu, *Anal. Chim. Acta,* 2012, **737**, 22.

54 Y. M. Wu, W. J. Xu, Y. Wang, Y. L. Yuan and R. Yuan, *Electrochim. Acta,* 2013, **88**, 135.

55 H. Wang, H. Li, Y. H. Zhang, Q. Wei, H. M. Ma, D. Wu, Y. Li, Y. 95 Zhang and B. Du, *Biosens. Bioelectron*., 2014, **53**, 305.